PHYSICAL REVIEW B **78**, 075304 (2008)

Anderson localization from classical trajectories

Piet W. Brouwer
Laboratory of Atomic and Solid State Physics, Cornell University, Ithaca, New York 14853, USA

Alexander Altland
Institut für Theoretische Physik, Zülpicher Strasse 77, 50937 Köln, Germany

(Received 7 February 2008; revised manuscript received 6 June 2008; published 5 August 2008)

We show that Anderson localization in quasi-one-dimensional conductors with ballistic electron dynamics, such as an array of ballistic chaotic cavities connected via ballistic contacts, can be understood in terms of classical electron trajectories only. At large length scales, an exponential proliferation of trajectories of nearly identical classical action generates an abundance of interference terms, which eventually leads to a suppression of transport coefficients. We quantitatively describe this mechanism in two different ways: the explicit description of transition probabilities in terms of interfering trajectories, and an hierarchical integration over fluctuations in the classical phase space of the array cavities.

DOI: 10.1103/PhysRevB.78.075304 PACS number(s): 05.45.Mt, 73.20.Fz, 73.23.−b

I. INTRODUCTION

The interplay of quantum phase coherence and repeated random scattering is at the origin of many effects in mesoscopic physics.[1,2] These effects include weak localization and universal conductance fluctuations, both of which are small but fundamental corrections with respect to the conductance obtained from Drude-Boltzmann theory. They culminate in Anderson localization, the phenomenon that the resistance of the majority of low dimensional electron systems grows exponentially with system size if the system is sufficiently large.[3–5]

Originally, Anderson localization and other mesoscopic effects were discovered in the context of disordered metals, in which electrons scatter off impurities with a size comparable to their wavelength. Theoretically, quantum effects in disordered metals are described using the "disorder average" which deals with an ensemble of macroscopically equivalent but microscopically different impurity configurations. The presence of impurities is not essential for the existence of quantum effects, however. The same effects, with the same statistical properties, have been found to appear if the electron motion is ballistic and chaotic, the only source of scattering of electrons being specular reflection off the sample boundaries.[6–8] Besides being of theoretical interest for understanding the quantum properties of systems with chaotic classical dynamics,[9] the case of ballistic electron motion is relevant experimentally for very clean artificially structured two-dimensional electron gases in semiconductor heterostructures, such as quantum dots or antidot lattices.[10–12]

Unlike disordered metals, in which impurities scatter diffractively, electrons in ballistic conductors have a well-defined classical dynamics. Many quantum properties of ballistic conductors with chaotic classical dynamics can be understood in terms of classical mechanics by making use of well-chosen semiclassical methods.[7,9] A well-known example is the Gutzwiller trace formula, which relates the density of states to properties of periodic orbits of the classical dynamics.[13] For the conductance G and its quantum corrections, there is a variant of Gutzwiller's formula (the origins of which are before Gutzwiller's work[14]), which expresses G as a double sum over classical trajectories α and β connecting the source and drain contacts,[6,15,16]

$$G = \frac{1}{2\pi\hbar}\int dp dp' \sum_{\alpha,\beta} A_\alpha A_\beta e^{i(S_\alpha - S_\beta)/\hbar}. \tag{1}$$

Upon entrance and exit, the trajectories α and β have the same transverse momenta p and p', respectively, but the position at which they enter or exit the sample may be different. Further, $A_{\alpha,\beta}$ and $S_{\alpha,\beta}$ are the so-called "stability amplitude" and the classical action of the trajectories.

With Eq. (1) as a starting point, the conductance, including its quantum corrections, can be calculated solely from knowledge of classical trajectories. Quantum effects have been linked to the existence of families of classical trajectories that only differ near "small-angle encounters" of the trajectory with itself.[17–21] This semiclassical approach has been very successful explaining quantum effects in the "perturbative regime" in which quantum interference provides a small correction to the classical mechanics.[17–20,22–26] Weak localization and universal conductance fluctuations are examples of such perturbative quantum effects. On the other hand, a direct evaluation of the summation over classical trajectories breaks down outside the perturbative regime because of a proliferation of trajectories with correlated classical actions. This limitation applies both for phenomena that involve times longer than the Heisenberg time $t_H = h/\Delta$, Δ being the mean level spacing in a finite-sized system, or system sizes larger than the localization length ξ, if the system exhibits Anderson localization.[27]

Recently, Heusler *et al.* showed that, nevertheless, it is possible to understand quantum effects in terms of classical trajectories outside the perturbative regime. They considered the spectral form factor $K(t)$ of a ballistic cavity, the Fourier transform of the two-point correlation function of the density of states. Although direct semiclassical evaluation of $K(t)$ using Gutzwiller's trace formula was known to be possible for $t < t_H$ only,[17,18,22,23,28,29] Heusler *et al.* used a different way to express $K(t)$ in terms of periodic orbits, motivated by

the field-theoretical formulation of the problem, that allowed them to calculate $K(t)$ for all times.[30]

In this article, we consider Anderson localization for ballistic electron gases, and show that it, too, can be understood in terms of interference of classical trajectories, with Eq. (1) as a starting point. Examples of systems that may exhibit such "ballistic Anderson localization" are antidot lattices or arrays of chaotic cavities. Although it is generally accepted that Anderson localization exists irrespective of the details of the microscopic electronic dynamics,[31] the similarity of the phenomena for ballistic and disordered electron systems should not obscure the vastly different starting points of the theories for the two cases. This difference not only pertains to the microscopic dynamics (classical deterministic vs quantum probabilistic), but also to the statistical assumptions of the theory. Unlike theories of quantum transport in disordered metals, semiclassical theories of ballistic conductors are intended to describe one specific system.[9] Fluctuations appear solely from variations of the Fermi energy; no changes in the classical dynamics are invoked. In this sense, our approach is very different from random matrix theory or other effectively stochastic theories.

For disordered metals, Anderson localization is the most prominent for a quasi-one-dimensional geometry, with sample length L much larger than the sample width W. For quasi-one-dimensional samples, a full theory of transport in the localized regime was developed by Dorokhov[32] and Mello *et al.*[33] using a stochastic approach, and by Efetov and Larkin,[34,35] using a field-theoretic approach. Our theory of ballistic Anderson localization closely follows these approaches. The fact that the semiclassical theory for ballistic electrons follows the corresponding quantum-mechanical theory for disordered metals is not special to the present case. It is also typical of the trajectory-based semiclassical theories in the perturbative regime, which have a structure that resembles the diagrammatic perturbation theory of quantum corrections in disordered metals.[17–19]

In addition to the ballistic electron gases considered here, Anderson localization also occurs in certain dynamic systems with a periodic time-dependent Hamiltonian, such as the kicked rotor.[9] Classically, the dynamics of the kicked rotor is chaotic, with a momentum that changes diffusively under the influence of the periodic kicks. Quantum mechanically, it exhibits "dynamic localization," Anderson localization in momentum space rather than in real space.[36] The phenomenology of dynamic localization is equal to that of Anderson localization in disordered metals. This is confirmed by extensive numerical simulations,[37,38] as well as a field-theoretical analysis of the problem.[39]

Previous trajectory-oriented work addressed localization in strictly one-dimensional geometries, such as single-channel wires[40] or one-dimensional quantum graphs.[41] These one-dimensional geometries behave differently from the quasi-one-dimensional ballistic conductors studied here. In one dimension, the condition of (nearly) identical phases of interfering semiclassical contributions is much less restrictive than in higher dimensions. This reflects in localization in one dimension being categorically strong—there is no such thing like "weak" one-dimensional localization. Technically, these differences show in the "topology" of relevant contributions to the double sum Eq. (1), or in a different scaling equation describing the incremental development of transport coefficients.[32,33] Specifically, in one dimension, two interfering trajectories scattering a given set of impurities may do so at any sequential order, provided the length of the trajectories stay identical (up to a wavelength). In higher dimensions, even for a quasi-one-dimensional geometry, phase-space restrictions remove this freedom; scattering paths have to be pairwise identical over extended segments much larger than the characteristic scattering lengths, l.[17–20,42] (A phenomenon that finds its quantitative expression in the so-called "noncrossing approximation" in theories of disordered electron systems in higher dimensions.) Only at lengths scales comparable to the localization length $\xi \gg l$, deviations from this rule gain importance, and it is the phase volume of these processes which we aim to describe in our present approach. This task is fundamentally different from the description of one-dimensional, strongly interfering scattering paths. (It may be worth noting that in the closely related context of disordered quantum wires, a semiclassical or diagrammatic solution of the strictly one-dimensional problem[40] was obtained more than a decade before the multichannel case was solved.[32,34,35])

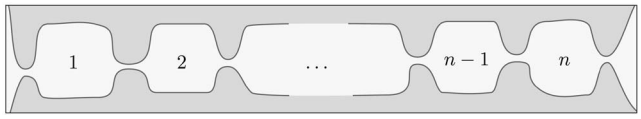

FIG. 1. Schematic of an array of n chaotic cavities. The cavities are connected via ballistic contacts with dimensionless conductance g_c. The semiclassical theory requires the limit $g_c \to \infty$ at a fixed ratio n/g_c.

The trajectory-based theory of ballistic Anderson localization that we report here is constructed for a specific system, an array of chaotic cavities. A schematic of such an array is shown in Fig. 1. We use this model system because the trajectory-based theory of transport through a single chaotic cavity is well established in the literature.[16,19,20,24,26,43,44] Arrays of cavities have been used as a starting point for a field-theoretic description of Anderson localization using random matrix theory,[45,46] but not with Dorokhov's method. In Sec. II, we show how Dorokhov's theory can be adapted to this system if the cavities are disordered, and random matrix theory can be used to describe transport through a single cavity. In Sec. III, we summarize the basic elements of the trajectory-based semiclassical formalism. This formalism is used to construct the trajectory-based semiclassical theory of ballistic localization in Sec. IV. In Sec. V, we approach the localization phenomenon from a different perspective. We describe the array in terms of a nonlinear σ model whose perturbative ("diagrammatic") evaluation generates structures of paired Feynman amplitudes similar to those appearing in the native semiclassical approach. Alternatively, the dynamical structure of the theory can be analyzed to identify and successively eliminate hierarchies of different types of dynamical fluctuations in the system. In this way we obtain an effective low energy theory which turns out to be equivalent to the nonlinear σ model of diffusive quantum wires; the latter model is known to predict exponential localization at large length scales. We conclude in Sec. VI.

II. ARRAY OF DISORDERED CAVITIES

We now describe how Dorokhov's approach can be used to describe Anderson localization in an array of disordered cavities or quantum dots. We take the disorder in each cavity to be weak (cavity size is much smaller than the localization length), so that transport through a single cavity is described by random matrix theory.[47]

A schematic of the array of cavities is shown in Fig. 1. The cavities are connected via ballistic contacts with dimensionless conductance g_c. Since we want to compare with a semiclassical theory for an array of ballistic cavities, we require $g_c \gg 1$. Localization takes place if the conductance of the array is of order unity. This condition is met if the number n of cavities in the array is comparable to g_c. Hence, in the calculations below we take the limit $g_c \to \infty$ while keeping the ratio n/g_c fixed. The same limit is taken in the field-theoretical description of localization,[34,35,45,46,48] where it is known as the "thick wire limit."

The transport properties of the array of cavities are encoded in its scattering matrix $S^q(n)$. (The superscript "q" is used to distinguish the quantum-mechanical scattering matrix from its semiclassical counterpart to be introduced in Sec. III.) The matrix indices of $S^q(n)$ represent the two contacts $i=1,2$ at the far left and right of the array and the transverse modes in each contact, $|p_{\perp,i}| = \pm \pi\hbar n_i/W$, $n_i = 1,2,\ldots,N$, where $N=g_c$ is the number of channels in contact i, $i=1,2$. The matrix $S^q(n)$ is a random quantity because it depends on the Fermi energy and on the precise disorder configuration in each cavity. Following the approach of Dorokhov[32] and Mello *et al.*,[33] we consider the Hermitian matrix

$$T^q(n) = S^q_{12}(n) S^{q\dagger}_{12}(n), \tag{2}$$

and calculate its statistical distribution by expressing $T^q(n)$ in terms of $T^q(n-1)$ and proceeding recursively. The matrix T^q is related to the dimensionless conductance $g(n)$ of the array through the Landauer formula,

$$g(n) = \mathrm{tr}\, T^q(n). \tag{3}$$

Taking the scattering matrix of each individual cavity from the circular ensemble of random matrix theory,[47] one then finds that the recursion relation for T^q takes the form

$$\delta T^q = T^q(n) - T^q(n-1) = -\frac{1}{g_c} T^q(n-1)\,\mathrm{tr}\, T^q(n-1) - \frac{1}{g_c}\delta_{\beta,1} T^q(n-1)^2 + X^q(n) + \mathcal{O}(g_c^{-3/2}), \tag{4}$$

where the Hermitian matrix X is a random (noise) term with a Gaussian distribution,

$$\langle X^q(n)_{ij}\rangle_n = 0,$$

$$\langle X^q(n)_{ij} X^q(n)_{kl}\rangle_n = \frac{1}{g_c} T^q(n-1)_{il} F^q_{kj} + \frac{1}{g_c} T^q(n-1)_{kj} F^q_{il} + \frac{2}{g_c}\delta_{\beta,1} G^q_{ij} G^{q*}_{kl}, \tag{5}$$

where $F^q = T^q(1-T^q)$, $\beta=1$ or 2 in the presence or absence of time-reversal symmetry, respectively, and

$$G^q = S^q_{12} S^{q\dagger}_{22} S^q_{21}. \tag{6}$$

The averaging brackets $\langle\ldots\rangle_n$ denote an average with respect to the disorder configuration in the nth cavity only.

In the limit $g_c \to \infty$ while keeping n/g_c fixed, the stochastic recursion relation (4) can be mapped to the Dorokhov-Mello-Pereyra-Kumar (DMPK) equation, which is a stochastic differential equation for the eigenvalues of T^q.[32,33,47,49] The solution of the DMPK equation is known,[47] which completes the theory of localization for an array of disordered cavities.

Alternatively, the stochastic recursion relation (4) can be used to generate a coupled set of recursion relations for the disorder averages of the moments of $T(n)$,

$$\delta\left\langle \prod_{m=1}^{n} T_{i_m}\right\rangle = \left\langle \prod_{m=1}^{n} T_{i_m}(n)\right\rangle - \left\langle \prod_{m=1}^{n} T_{i_m}(n-1)\right\rangle = -\frac{1}{g_c}\delta_{\beta,1}\sum_{k=1}^{n} i_k \left\langle T_{i_k+1}\prod_{\substack{m=1\\ m\neq k}}^{n} T_{i_m}\right\rangle - \frac{1}{g_c}\left(\sum_{k=1}^{n} i_k\right)\left\langle T_1\prod_{m=1}^{n} T_{i_m}\right\rangle + \frac{1}{g_c}\sum_{k=1}^{n}\sum_{j=1}^{i_k-1} i_k \left\langle (T_j(T_{i_k-j} - T_{i_k-j+1}))\prod_{\substack{m=1\\ m\neq k}}^{n} T_{i_m}\right\rangle + \frac{4}{\beta g_c}\sum_{k=1}^{n}\sum_{l=1}^{k-1} i_k i_l \left\langle (T_{i_k+i_l} - T_{i_k+i_l+1})\prod_{\substack{m=1\\ m\neq k,l}}^{n} T_{i_m}\right\rangle + \mathcal{O}(g_c^{-2}), \tag{7}$$

with

$$T_m = \mathrm{tr}(T^q)^m. \tag{8}$$

(The argument $n-1$ is suppressed on the right-hand side of the second equality.) The average in Eq. (7) is the full disorder average, applied to all cavities in the array. Taking the limit $g_c \to \infty$ at fixed n/g_c, Eq. (7) is mapped to a coupled set of differential equations for the moments of T^q which is identical to the corresponding set of differential equations for a disordered wire.[50,51] A subset of these equations can be resummed into a partial differential equation for the generating function F_β, with[46,52]

$$F_1 = \left\langle \det \prod_{\pm} \left(\frac{2 + (\cos(\theta_3) - 1)T^q}{2 + (\cosh(\theta_1 \pm \theta_2) - 1)T^q} \right)^{1/2} \right\rangle,$$

$$F_2 = \left\langle \det \left(\frac{2 + (\cos(\theta_3) - 1)T^q}{2 + (\cosh(\theta_1) - 1)T^q} \right) \right\rangle. \quad (9)$$

As shown in Refs. 46 and 52, the resulting theory of localization in quasi-one-dimension is formally equivalent to that obtained from the one-dimensional nonlinear sigma model.[34,35,45,48]

III. SEMICLASSICAL FORMALISM

The central object in the trajectory-based semiclassical theory of localization in an array of ballistic chaotic cavities is a semiclassical representation of the scattering matrix S^q. In the semiclassical representation, the discrete transverse momenta become continuous variables, so that the scattering matrix S^q becomes a "scattering kernel" $S_{ij}(p',p)$.[53] Following standard semiclassical approximations, this scattering kernel is then represented as a sum over classical trajectories α connecting contact j to contact i,[6,14–16]

$$S_{ij}(p',p) = \frac{1}{\sqrt{2\pi\hbar}} \sum_{\alpha} A_\alpha e^{iS_\alpha/\hbar}, \quad (10)$$

such that the transverse momentum of α upon entrance and exit equals p and p', respectively. Further, S_α is the classical action of α, and A_α is the stability amplitude,

$$A = \left| \frac{\partial p'}{\partial q} \right|^{-1/2}, \quad (11)$$

where q is the transverse position upon entrance into the sample. Maslov indices and other additional phase shifts are included in S_α. (Since Maslov indices do not enter into action differences between nearby trajectories, they do not play an essential role in the considerations that follow.) Because the transverse modes in the quantum-mechanical formulation are linked to the absolute value of the transverse momentum, not to the transverse momentum itself, the semiclassical counterpart of the products $S_{ij}S^\dagger_{kj}$ and $S^\dagger_{jk}S_{ji}$ consist of two contributions: one in which transverse momenta in contact j are equal and one in which the transverse momenta are opposite,

$$[S_{ij}S^\dagger_{kj}](p',p) = \sum_{\pm} \int_{-p_F}^{p_F} dp'' S_{ij}(p',p'') S^\dagger_{kj}(p, \pm p''),$$

$$[S^\dagger_{jk}S_{ji}](p',p) = \sum_{\pm} \int_{-p_F}^{p_F} dp'' S^\dagger_{jk}(\pm p'',p') S_{ji}(p'',p), \quad (12)$$

Together, Eqs. (10) and (12) specify how products of the quantum-mechanical scattering matrix and its Hermitian conjugate are expressed in terms of classical trajectories. [The "–" terms in the summations were omitted from the semiclassical expression for the conductance, Eq. (1) above.]

For a theory of Anderson localization, we are interested in the trace of a product of alternating factors S and $S^\dagger$ or in the product of such traces. Using the semiclassical representation (10), a polynomial function $F(S,S^\dagger)$ that involves the alternating product of n factors S and n factors $S^\dagger$ is written as a summation over $2n$ classical trajectories $\alpha_1,\ldots,\alpha_n$ and $\beta_1,\ldots,\beta_n$, one trajectory for each factor S or $S^\dagger$, respectively. Each configuration of classical trajectories is weighed by a phase factor $\exp(i\Delta S/\hbar)$ with

$$\Delta S = \sum_{i=1}^{n} S_{\alpha_i} - \sum_{i=1}^{n} S_{\beta_i}. \quad (13)$$

Building on work by Richter and Sieber,[17–19] Haake and coworkers have identified a hierarchy of families of classical trajectories $\alpha_1,\ldots,\beta_n$ that contribute to the average $\langle F\rangle$,[20,22–24] where the average is taken with respect to variations of the Fermi energy while keeping the classical dynamics (i.e., the shape of the cavities) fixed. Their identification is based on the recognition that families of trajectories contribute to $\langle F\rangle$ only if their total action difference ΔS is of order $\hbar$ *systematically*, which happens only if the trajectories α_i are piecewise and pairwise identical to the trajectories β_j, $i,j=1,\ldots,n$, up to classical phase-space distances of order $\hbar^{1/2}$.[17,18] Families of trajectories that are separated by larger phase-space distances have typical action differences ΔS that are parametrically larger than $\hbar$, so that their contribution vanishes upon taking the average. (The condition that the total action difference ΔS be of order $\hbar$ systematically means that ΔS must remain small if the trajectories are continuously deformed.)

The simplest choice for a family of trajectories for which ΔS is of order $\hbar$ systematically is if each trajectory α_i equals another trajectory β_j for the full length of the trajectory. Calculating $\langle F\rangle$ from the contribution from such families of trajectories only is known as the "diagonal approximation."[16,43,44] Nontrivial families of trajectories emerge from the possibility of small-angle encounters between trajectories, at which more than two trajectories are within a phase-space distance $\sim\hbar^{1/2}$.[42] At such small-angle encounters, the pairing between the α_i and β_j can be changed—so that now trajectories need to be piecewise identical only. The duration of a small-angle encounter is the "Ehrenfest time" $\tau_E=\lambda^{-1}\ln(p_F l/\hbar)$, where λ is the Lyapunov exponent of the classical dynamics, p_F is the Fermi momentum, and l a characteristic length scale of the classical dynamics. The fundamental action integrals corresponding to each small-angle encounter are known,[22,23,54,55] and the resulting theory takes the form of simple combinatorial rules with which any product of traces of products the scattering matrix and its Hermitian conjugate can be calculated to arbitrary order in $\hbar$ from the semiclassical representation of S, provided that the Ehrenfest time τ_E be much smaller than the sample's mean dwell time τ_D.[20,22–24] (The case of finite τ_E/τ_D is considerably more complicated, see, e.g., Refs. 25, 26, 56, and 57, but not relevant for a semiclassical theory of Anderson localization.)

In the remainder of this text, we refer to a calculation of the energy-average $\langle F\rangle$ using contributions from families of trajectories thus constructed as the "trajectory-based semiclassical formalism." Although there is no formal proof that this formalism is exact, i.e., that there are no other contribu-

tions to $\langle F\rangle$ than from families of piecewise paired classical trajectories, the formalism satisfies all known conservation rules, and calculations based on trajectory-based semiclassics have been found to agree with fully quantum-mechanical calculations whenever applicable.[20,57] The present calculation can be viewed as another demonstration of the validity of trajectory-based semiclassics by showing that the same formalism can serve as the starting point of a theory of localization.

While we do not need the detailed results of the trajectory-based semiclassical formalism, there are two properties of ensemble averages calculated using this formalism that are particularly relevant for our calculations below:

(i) All averages are compatible with the condition of unitarity,[20]

$$\sum_j [S_{ij}S_{kj}^\dagger](p,p') = \sum_j [S_{jk}^\dagger S_{ji}](p,p') = \delta_{ik}\delta(p-p'). \tag{14}$$

(ii) For a product $S_{ij}S_{kj}^\dagger$ or $S_{ji}^\dagger S_{jk}$, the trajectory α of the semiclassical representation for S and the trajectory β of the semiclassical representation of $S^\dagger$ at contact j satisfy

$$p_\alpha = p_\beta, \quad |q_\alpha - q_\beta| \lesssim \hbar/p_F. \tag{15}$$

In particular, this implies that there is no contribution from the second term in Eq. (12) for a product of two scattering kernels.[25,56]

Property (ii) follows from the requirement that the net action difference ΔS to be of order $\hbar$ *systematically*. This means that ΔS should remain of order $\hbar$ if one (continuously) deforms the trajectories. Deformed trajectories have different transverse momenta p and p' or transverse positions q and q' in the entrance and exit contacts, but they remain (exponentially) close to the original trajectory in the sample interior. If condition (ii) is not met, the sum over all deformations of a certain set of trajectories contains a rapidly oscillating phase factor, which suppresses the contribution to the average, even if the action difference ΔS happens to be small for a particular set of trajectories in the sum.

IV. ARRAY OF BALLISTIC CAVITIES

In the perturbative regime, the semiclassical theories of quantum corrections to transport and to the density of states closely followed the corresponding theory for disordered metals. The semiclassical formalism described in the Sec. III was instrumental in formalizing the relation between the two types of theories. Motivated by this correspondence, we now look for the possibility to adapt the theory of localization in an array of disordered cavities (Sec. II) to the case of an array of ballistic cavities.

Thus, paraphrasing the arguments of Sec. II, the goal of our calculation will be to find the full probability distribution of the function

$$T(n;p',p) = [S_{12}S_{12}^\dagger](p',p) \tag{16}$$

for an array of n cavities. As shown in Sec. II, there are two ways in which this can be accomplished:

(1) Using a stochastic approach, in which one considers the stochastic evolution of the function $T(n;p',p)$ as a function of n, or through

(2) the construction of a set of recursion relations for all moments of $T(n)$.

In both cases, the resulting theory is formally identical to the known theories of localization in quasi-one-dimension.

Although technically simpler, the stochastic approach is at odds with the goals of a semiclassical theory for ballistic localization; the goal of a theory of localization in an array of ballistic cavities is to describe an array of cavities with a fixed shape, using variations of the Fermi energy as the only source of statistical fluctuations. Since the Fermi energy is set globally, for all cavities at the same time, quantum corrections for different cavities are not independent, and a stochastic approach is ruled out *a priori*. A stochastic approach is possible, however, if one relaxes the goals of the theory, allowing for small variations of the shape of each cavity, or for variations of a "gate voltage" that sets the Fermi energy of each cavity independently.

Below we first describe the stochastic approach. In Section IV A, we consider the case of broken time-reversal symmetry, which is technically simpler. The discussion of localization in the presence of time-reversal symmetry is given in Sec. IV B. In Sec. IV C, we discuss how a hierarchy of recursion relations for the moments of T can be constructed, where the average is taken with respect to variations of the Fermi energy of the entire array only.

A. Stochastic approach

The stochastic approach deals with (statistical) properties of the function $T(n)$ before averaging. Although the properties (i) and (ii) of the trajectory-based semiclassical formalism (Sec. III) are satisfied for the average of *any* product of traces of products alternating factors S and $S^\dagger$ to arbitrary order in $\hbar$, they have not been shown to follow from the semiclassical scattering matrix [Eq. (10)] *before* averaging. However, since our goal is a statistical theory of the transport—the final statements of the theory will refer to averaged quantities only—we will accept these two properties on the level of the sample-specific semiclassical scattering kernel $S(n;p',p)$ in the arguments that follow below.

Starting from Eq. (10), the kernel T is expressed as a double sum over classical trajectories α and β that connect the entrance and exit contacts (Fig. 2),

$$T(p',p) = \sum_{\alpha,\beta} \frac{A_\alpha A_\beta}{2\pi\hbar} e^{i(S_\alpha - S_\beta)/\hbar}. \tag{17}$$

Here p and p' are the transverse momenta of α and β upon entrance. The two trajectories have equal transverse momenta upon exit, and exit at positions a quantum uncertainty $\sim\hbar/p_F$ apart—see property (ii) above. Below, we express the difference $\delta T = T(n) - T(n-1)$ in terms of classical trajectories. We first calculate the average $\langle \delta T\rangle_n$, where the average is taken with respect to variations of the Fermi energy of the nth cavity (or of its shape), while keeping the Fermi energy and shape of the other cavities fixed. After that, we calculate the variance of δT and the higher cumulants.

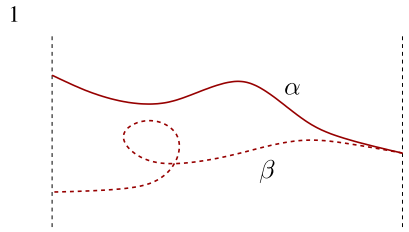

FIG. 2. (Color online) Example of a pair of trajectories α and β contributing to $T(p',p)=[S_{12}S_{12}^{\dagger}](p',p)$. Upon entering the sample, the two trajectories have different transverse momenta p and q, and may enter at different transverse positions. Upon exiting the sample, α and β have the same transverse momentum, and exit at transverse positions a distance $\lesssim\hbar/p_F$ apart.

Average of δT. When calculating the average $\langle\delta T\rangle_n=\langle T(n)\rangle_n-T(n-1)$ to leading order in $1/g_c$ in the absence of time-reversal symmetry, it will be sufficient to calculate $\langle T(n)\rangle_n$ in the diagonal approximation by considering trajectories α and β that are "paired" in the nth cavity. Note, however, that trajectories need not be paired in the first $n-1$ cavities, because no average is taken there. Each trajectory is classified by the number of times m_α, m_β that it enters the nth cavity from the $(n-1)$th cavity. Hence, for each trajectory there are m_α and m_β segments in the nth cavity, which we label as $\alpha_1,\ldots,\alpha_{m_\alpha}$ and $\beta_1,\ldots,\beta_{m_\beta}$. Since trajectories are paired in the nth cavity, $m_\alpha=m_\beta=m$. Examples of trajectory pairs α and β with $m=1$, 2, and 3 are shown in Fig. 3. Since trajectories need to be paired upon exit, α_m has to be paired with β_m. While there are $(m-1)!$ ways in which the remaining segments can be paired, we now show that the "diagonal pairing," α_j paired with β_j, $j=1,\ldots,m$, gives the main contribution to $\langle\delta T\rangle_n$, whereas all other pairings give contributions a factor $1/g_c$ smaller.

Cutting the trajectories α and β at the contact between the $(n-1)$st and nth cavity also separates the part of each trajectory that resides in the first $n-1$ cavities into m segments. The first segment of each trajectory connects the entrance contact to the exit of the $(n-1)$st cavity. All other segments connect the exit contact of the $(n-1)$st cavity to itself. Since the electron dynamics in the nth cavity is fully ergodic, the positions and transverse momenta with which these segments cross the interface between the $(n-1)$st and nth cavity are fully random, without correlations between different segments. [Correlations can be ruled out down to quantum phase-space distances $\sim\hbar/(p_FL)^{1/2}$ because the dwell time $\tau_D\gg\tau_E$.] Hence, these m segments can be interpreted as the semiclassical representation of a product of S_{12}, $S_{12}^{\dagger}$, and $m-1$ factors S_{22} and $S_{22}^{\dagger}$, *before* taking any average. Note that, although trajectories α,β that are "paired" in the nth cavity have a phase-space distance of order $\hbar/(p_FL)^{1/2}$ or smaller when they enter/exit the nth cavity from/to the $(n-1)$st cavity, such trajectory pairs are sufficient for the semiclassical calculation of the complete kernels T because of property (ii) of Sec. III.

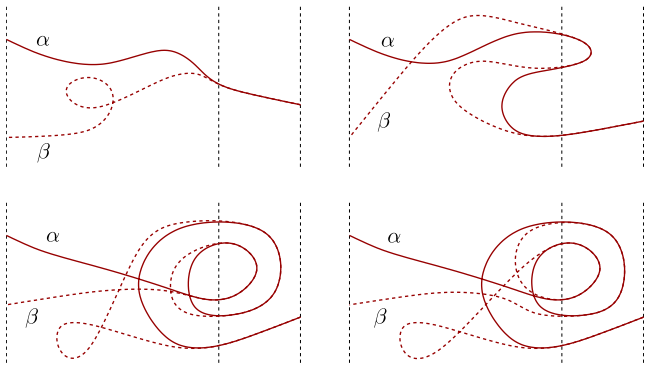

FIG. 3. (Color online) Examples of trajectories α and β contributing to $\langle T(n)\rangle_n$, where an average is taken over the Fermi energy of the nth cavity only. The four panels show trajectories contributing for $m=1$ (top left), $m=2$ (top right), $m=3$ with diagonal pairing (bottom left), and $m=3$ with nondiagonal pairing (bottom right). The number m counts the number of times α and β enter the nth cavity from the $(n-1)$st cavity. The three dashed lines in each panel represent the entrance contact, the contact between the $(n-1)$st cavity and the nth cavity, and the exit contact (from left to right). In the nth cavity, the trajectories α and β are piecewise equal up to quantum uncertainties.

For the diagonal pairing, the m segments of α and β that reside in the first $n-1$ cavities generate a particularly simple product of factors S and $S^{\dagger}$, $T(n-1)[\mathrm{tr}\,R(n-1)]^{m-1}$, where

$$R(n;p,p')=[S_{22}(n)^{\dagger}S_{22}(n)](p,p') \tag{18}$$

is the reflection coefficient for the first $n-1$ cavities, seen from the exit contact of the $(n-1)$st cavity, and

$$\mathrm{tr}\,R(n)=\int_{-p_F}^{p_F}dpR(n;p,p). \tag{19}$$

Using the trajectory-based semiclassical formalism to evaluate the diagonal trajectory sums in the nth cavity,[19,20,24,43,44] one then easily finds that the diagonal pairing gives

$$\langle T(n)\rangle_n=\sum_{m=1}^{\infty}\frac{1}{2^m g_c^{m-1}}T(n-1)[\mathrm{tr}\,R(n-1)]^{m-1}$$

$$=\frac{T(n-1)g_c}{2g_c-\mathrm{tr}\,R(n-1)}. \tag{20}$$

Using unitarity, one has

$$\mathrm{tr}\,R(n)=g_c-\mathrm{tr}\,T(n), \tag{21}$$

so that Eq. (20) can be rewritten as

$$\langle\delta T\rangle_n=-\frac{1}{g_c}T(n-1)\mathrm{tr}\,T(n-1), \tag{22}$$

up to corrections of order $1/g_c^2$. This is precisely the semiclassical equivalent of the recursion relation of Eq. (4), averaged over the Fermi energy or shape of the nth cavity.

It remains to show that nondiagonal pairings, in which a segment α_j is not paired with β_j give a contribution to $\langle\delta T\rangle_n$ that can be neglected in the limit of large g_c. Hereto, we first consider the case $m=3$, for which the only possible nondiagonal pairing is $\alpha_1\leftrightarrow\beta_2$, $\alpha_2\leftrightarrow\beta_1$ (Fig. 3, bottom right). For this pairing, the three segments of the trajectories that reside in the first $n-1$ cavities generate the semiclassical representation of a product of six scattering matrices, $S_{12}S_{22}^{\dagger}S_{22}S_{22}^{\dagger}S_{22}S_{12}^{\dagger}$. From unitarity, one has

$$S_{12}S_{22}^{\dagger}S_{22}S_{22}^{\dagger}S_{22}S_{12}^{\dagger} = T(n-1) - 2T(n-1)^2 + T(n-1)^3. \tag{23}$$

For comparison, the diagonal pairing for $m=3$ generates $T(n-1)[\mathrm{tr}\, R(n-1)]^2$, which is a factor $\sim g_c^2$ larger because $\mathrm{tr}\, R(n-1) \sim g_c$. Using the ergodic dynamics in the nth cavity, the nondiagonal pairing of segments in the nth cavity for $m=3$ gives a contribution to $\langle \delta T\rangle_n$ equal to

$$\langle \delta T\rangle_n^{(3,\mathrm{non\ diag})} = \frac{1}{8g_c^2}[T(n-1) - 2T(n-1)^2] + T(n-1)^3. \tag{24}$$

This is a factor $\sim 1/g_c$ smaller than the leading contribution [Eq. (22)] to $\langle \delta T\rangle_n$.

The same arguments can be used for $m>3$: Nondiagonal pairings come at the expense of at least two factors $\mathrm{tr}\, R(n-1)$ and, hence, lead to contributions to $\langle \delta T\rangle_n$ that are at least a factor $\sim 1/g_c$ smaller than the contribution from diagonal pairing. These arguments can also be used to show that contributions to $\langle T(n)\rangle_n$ that involve small-angle intersections of the trajectories in the nth cavity are a factor $1/g_c$ smaller than the leading contribution considered above.

Fluctuations of δT. The fluctuations of δT are described by the covariance $\langle \delta T(p_1,p_2)\delta T(p_1',p_2')\rangle_n$. We calculate $\langle \delta T(p_1,p_2)\delta T(p_1',p_2')\rangle_n$ from the identity

$$\langle \delta T\delta T'\rangle_n = \langle \delta(TT')\rangle_n - T(n-1)\langle \delta T'\rangle_n - T'(n-1)\langle \delta T\rangle_n, \tag{25}$$

where we used the shorthand notation $T(n)=T(n;p_1,p_2)$, $T'(n)=T(n;p_1',p_2')$, and $\delta(TT')=T(n)T'(n)-T(n-1)T'(n-1)$. The average $\langle \delta T\rangle_n$ is given by Eq. (22) above, so it remains to calculate $\langle \delta(TT')\rangle$. The product $T(n)T'(n)$ is represented as a sum over four classical trajectories, α, β, α', and β'. As before, we introduce the numbers m_α, m_β, $m_{\alpha'}$, and $m_{\beta'}$ that indicate how often each trajectory enters the nth cavity. Since trajectories always enter or exit the nth cavity in pairs, one has $m_\alpha+m_{\alpha'}=m_\beta+m_{\beta'}$.

Unlike the average $\langle \delta T\rangle_n$, for which the only contribution came from the diagonal approximation in the nth cavity with diagonal pairing of the segments α_j and β_j, the average of the second moment $\langle(\delta TT')\rangle_n$ has contributions from both nondiagonal pairings in the diagonal approximation and from trajectories beyond the diagonal approximation, which have small-angle encounters in the nth cavity. We first consider the diagonal approximation, for which each segment α_i or α_i' is paired with another segment β_j or β_j'. For the diagonal pairing of segments, $\alpha_j \leftrightarrow \beta_j$, $j=1,\ldots,m_\alpha=m_\beta$ and $\alpha_j' \leftrightarrow \beta_j'$, $j=1,\ldots,m_{\alpha'}=m_{\beta'}$, we find

$$\langle \delta(TT')\rangle_n^{\mathrm{diag}} = T(n-1)\langle \delta T'\rangle_n + T'(n-1)\langle \delta T\rangle_n. \tag{26}$$

This contribution to $\langle \delta T\delta T'\rangle_n$ precisely cancels the second and third terms in Eq. (25). Hence $\langle \delta T\delta T'\rangle_n$ must be from nondiagonal pairings of the trajectory segments within the diagonal approximation, or from trajectory configurations beyond the diagonal approximation in the nth cavity. Since the latter class of trajectories have small-angle encounters, we write

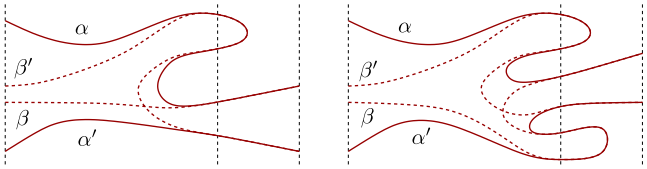

FIG. 4. (Color online) Examples of four trajectories α, β, α', and β' contributing to $\langle T(n;p',p)T(n;p'',p')\rangle_n$ for an array of chaotic cavities, where the average is taken with respect to the Fermi energy of the nth cavity only. The examples shown here have a nondiagonal pairing with $m_\alpha=m_{\beta'}=2$, $m_{\alpha'}=m_\beta=1$ (left panel) and $m_\alpha=m_{\beta'}=m_{\alpha'}=m_\beta=2$ (right panel). In the nth cavity, the trajectories α and α' are piecewise equal to β and β', up to quantum uncertainties.

$$\langle \delta T\delta T'\rangle_n = \langle \delta(T)\rangle_n^{\mathrm{non\ diag}} + \langle \delta(TT')\rangle_n^{\mathrm{enc}}. \tag{27}$$

The leading nondiagonal pairing appears if one pairs the first u segments of α with the first u segments of β', and the last $m_\alpha-u$ segments of α with the last $m_\alpha-u$ segments of β, as well as the first v segments of α' with the first v segments of β, and the last $m_{\alpha'}-v$ segments of α' with the last $m_{\alpha'}-v$ segments of β', where $u=1,\ldots,m_\alpha-1$ and $v=1,\ldots,m_\alpha'-1$ are integers. Two examples, with $m_\alpha=2$, $m_{\alpha'}=1$, $u=1$, and $v=0$, and with $m_\alpha=m_{\alpha'}=2$ and $u=v=1$, are shown in Fig. 4. One then finds

$$\langle \delta T\delta T\rangle_n^{\mathrm{non\ diag}} = \frac{1}{g_c}[F(p_1',p_2)T(p_1,p_2') + F(p_1,p_2')T(p_1',p_2) + T(p_1,p_2')T(p_1',p_2)] + \mathcal{O}(1/g_c^2), \tag{28}$$

where $T(p_1,p_2)=T(n-1;p_1,p_2)$ and $F(p_1,p_2)=F(n-1;p_1,p_2)$, with

$$F(n) = \mathrm{tr}\, S_{12}S_{22}^{\dagger}S_{22}S_{12}^{\dagger} = T(n) - T(n)^2. \tag{29}$$

Other pairings give contributions of order $1/g_c^2$ or smaller.

The second contribution to the fluctuations of δT comes from trajectories with a small-angle encounter in the nth cavity. Since we only need fluctuations of δT to leading order in $1/g_c$, it is sufficient to consider trajectories with one small-angle encounter only. Taking the small-angle encounter to be between the segments α_u, ${\beta'}_u$, ${\alpha'}_v$, and ${\beta'}_v$, with $1\le u, v \le m,m'$, and pairing the first $u-1$ segments of α with the first $u-1$ segments of β', and the last $m-u$ segments of α with the last $m-u$ segments of β, as well as the first $v-1$ segments of α' with the first $v-1$ segments of β, and the last $m'-v$ segments of α' with the last $m'-v$ segments of β', we find

$$\langle \delta T\delta T\rangle_n^{\mathrm{enc}} = -T(p_1,p_2')T(p_1',p_2)\sum_{u,v=1}^{\infty}\sum_{m=u}^{\infty}\sum_{m'=v}^{\infty}\frac{(\mathrm{tr}\, R)^{m+m'-2}}{2^{m+m'+1}g_c^{m+m'-1}} + T(p_1,p_2')T(p_1',p_2)\sum_{m=1}^{\infty}\sum_{m'=1}^{\infty}\frac{(\mathrm{tr}\, R)^{m+m'-2}}{2^{m+m'}g_c^{m+m'-1}} = -\frac{1}{g_c}T(p_1,p_2')T(p_1',p_2), \tag{30}$$

where the first line comes from encounters in the interior of

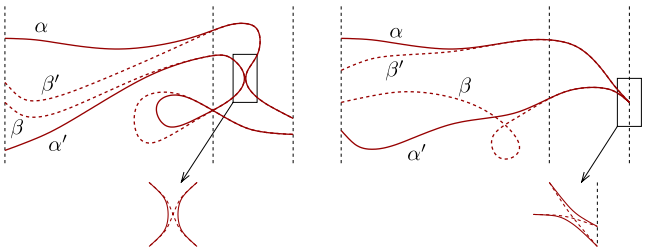

FIG. 5. (Color online) Two examples of a set of four trajectories contributing to $\langle TT' \rangle_n$ that have a small-angle encounter in the nth cavity. For the left panel, the encounter is in the interior of the nth cavity. For the right panel, it touches the exit contact.

the nth cavity and the second line comes from encounters that touch the exit contact.[25,58] Examples of the two terms for $m=m'=1$ are shown in Fig. 5. [We do not need to consider encounters that touch the contact between the $(n-1)$st cavity and the nth cavity, because the contribution from such encounters is included in the (products) of the kernel T of the first $n-1$ cavities.]

Combining everything we have

$$\langle \delta T(p_1,p_2)\delta T(p_1',p_2')\rangle_n = \frac{1}{g_c}[F(p_1',p_2)T(p_1,p_2') + F(p_1,p_2')T(p_1',p_2)] + \mathcal{O}(1/g_c^2). \tag{31}$$

Equation (31) is the semiclassical equivalent of Eq. (5).

Higher cumulants of δT can be calculated in the same way. For the kth cumulant, one finds that only pairings that involve trajectories out of all k factors T contribute. Each additional factor T involved in the pairing scheme contributes an additional factor $1/g_c$, which is why all cumulants with $k>2$ are of subleading order in $1/g_c$.

Together, Eqs. (22) and (31) form the semiclassical equivalent of the stochastic recursion relation (4) used in the fully quantum-mechanical theory of localization in disordered quasi-one-dimensional wires. The two moments describe the evoution of transport coefficients in the system. In the "semiclassical limit" ($g_c\to\infty$ while keeping g_c/n fixed), and in perfect analogy to the stochastic approach to quantum transport reviewed in Sec. II, this information reduces to the scaling equation of Dorokhov, Mello, Pereyra, and Kumar (DMPK).[32,33,47] The mapping onto the DMPK equation is proof of localization in arrays of chaotic cavities. It demonstrates that the transport characteristics of our system are equivalent to those of disordered quantum wires. The approximations used in this construction are stabilized by taking the semiclassical limit, and all have a one-to-one counterpart in the localization theory of disordered systems.

B. Presence of time-reversal symmetry

In the presence of time-reversal symmetry, both the average $\langle \delta T\rangle_n$ and the covariance $\langle \delta T \delta T'\rangle_n$ are different. In both cases, the difference appears because one can pair time-reversed trajectories when taking the ensemble average in the nth cavity.

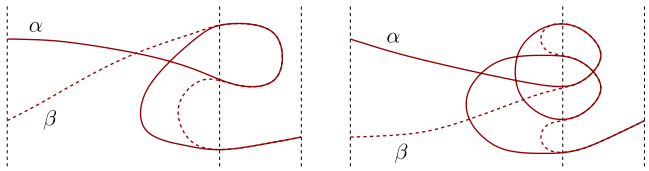

FIG. 6. (Color online) Two examples of trajectory pairs contributing to $\langle \delta T\rangle_n$ in the presence of time-reversal symmetry.

There are two additional contributions to the average $\langle \delta T\rangle_n$. The first of these arises from the diagonal approximation for the average in the nth cavity. As before, we define the number $m=m_\alpha=m_\beta$ as the number of times the trajectories α and β enter the nth cavity from the $(n-1)$st cavity. The first additional contribution to $\langle \delta T\rangle_n$ then involves the pairing of segments α_{u+j} with the time reversed of $\beta_{u+v-j-1}$, $j=0,\ldots,v-1$, and $1\le u\le u+v<m$,

$$\langle \delta T\rangle_n^{(1)} = F\sum_{v=1}^{\infty}\sum_{m=v+1}^{\infty}\frac{1}{2^m g_c^{m-1}}(\mathrm{tr}\, R)^{m-2} + T\sum_{u=1}^{\infty}\sum_{v=1}^{\infty}\sum_{m=u+v+1}^{\infty}\frac{\mathrm{tr}\, R^2}{2^m g_c^{m-1}}(\mathrm{tr}\, R)^{m-3} = \frac{1}{g_c}(F+T). \tag{32}$$

Examples for trajectory pairs contributing to the first and second line in Eq. (32) are shown in Fig. 6. The second contribution comes from small-angle encounters inside nth cavity involving the segments α_u, β_u, α_{u+v}, and β_{u+v}, where $1\le u\le u+v\le m$. For this contribution one finds

$$\langle \delta T\rangle_n^{(2)} = -\frac{2}{g_c}T. \tag{33}$$

Examples of trajectory pairs contributing to $\langle \delta T^{(2)}\rangle_n$ are shown in Fig. 7. Using $F=T-T^2$ and adding these two contributions to Eq. (22) one finds

$$\langle \delta T\rangle_n = -\frac{1}{g_c}T(n-1)\mathrm{tr}\, T(n-1) - \frac{1}{g_c}T^2, \tag{34}$$

up to corrections of order $1/g_c^2$.

For the fluctuations of δT in the presence of time-reversal symmetry one finds an extra contribution from pairing α_j with the time reversed of β'_{u+1-j}, $j=1,\ldots,u$, or α'_j with the

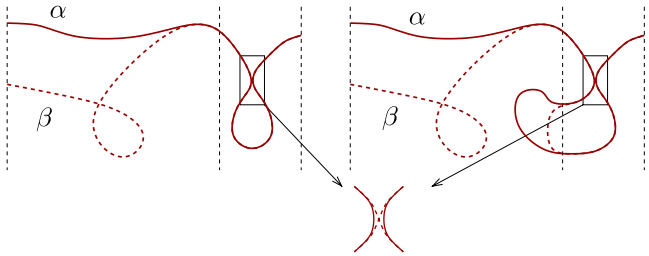

FIG. 7. (Color online) Two examples of trajectory pairs contributing to $\langle \delta T\rangle_n$ in the presence of time-reversal symmetry. The trajectory pairs have a small-angle encounter in the nth cavity.

time reversed of β_{u+1-j}, while following diagonal pairing rules for all other segments. Proceeding as before, we find

$$\langle \delta T(p_1,p_2)\delta T(p_1',p_2')\rangle_n = \frac{1}{g_c}[F(p_1',p_2)T(p_1,p_2') + F(p_1,p_2')T(p_1',p_2) + 2G(p,p_1')G^\dagger(p_2,p_2')] + \mathcal{O}(1/g_c^2). \tag{35}$$

where

$$G(p,p') = G(p',p) = [S_{12}S_{22}^\dagger S_{21}](p,p'). \tag{36}$$

The stochastic process defined by Eqs. (34) and (35) precisely mirrors the stochastic process (4) for the quantum-mechanical matrix $T^q = S_{12}^q S_{12}^{q\dagger}$.

C. Recursion relations for the moments of T

The direct construction of recursion relations for the moments of T is an alternative to the stochastic approach that avoids extending the use of the properties (i) and (ii) of Sec. III to sample-specific quantities and the necessity to define a statistical ensemble by varying the Fermi energy or shape of each cavity individually. The construction of recursion relations for moments of T proceeds in the very same manner as the construction of the stochastic recursion relations for T, with the additional requirement that trajectories are piecewise paired in all n cavities, not only in the nth cavity. Since the arguments of Secs. IV A and IV B did not rely on the structure of the trajectories in the first $n-1$ cavities, one immediately concludes that the recursion relations for the moments of T derived this way are identical to the recursion relations for the moments of T one obtains from the stochastic approach. Starting from the stochastic recursion relations (22) and (31) or (34) and (35), one arrives at the same hierarchy of recursion relations (7) derived for an array of disordered cavities.

We illustrate this procedure for the recursion relation for the first moment $\langle \mathrm{tr}\, T(n)\rangle$ in the absence of time-reversal symmetry. Following the rules of the semiclassical formalism, the average $\langle \mathrm{tr}\, T(n)\rangle$ is determined by trajectory pairs α, β that are piecewise paired throughout the entire array of cavities. The trajectories can have small-angle self-encounters, at which the pairing between α and β can be changed. Each pair of trajectories is classified by the number m of times the trajectories enter the nth cavity from the $(n-1)$st cavity. The m segments of each trajectory in the nth cavity are labeled $\alpha_1,\ldots,\alpha_m$ and $\beta_1,\ldots,\beta_m$.

As in Sec. IV A, it will be sufficient to consider pairs of trajectories in which each segment α_j is paired with the corresponding segment β_j, $j=1,\ldots,m$. Trajectory pairs with self-encounters in the nth cavity or with nondiagonal pairings in the nth cavity give contributions to $\delta\langle \mathrm{tr}\, T\rangle$ that are a factor $1/g_c$ smaller than the leading contribution. For the diagonal pairing, the remaining m segments of the trajectories α and β that reside in the first $n-1$ cavities precisely generate $\langle \mathrm{tr}\, T(n-1)[\mathrm{tr}\, R(n-1)]^{m-1}\rangle$, where the averaging brackets refer to variations of the Fermi energy for the entire array of cavities. Hence, we find

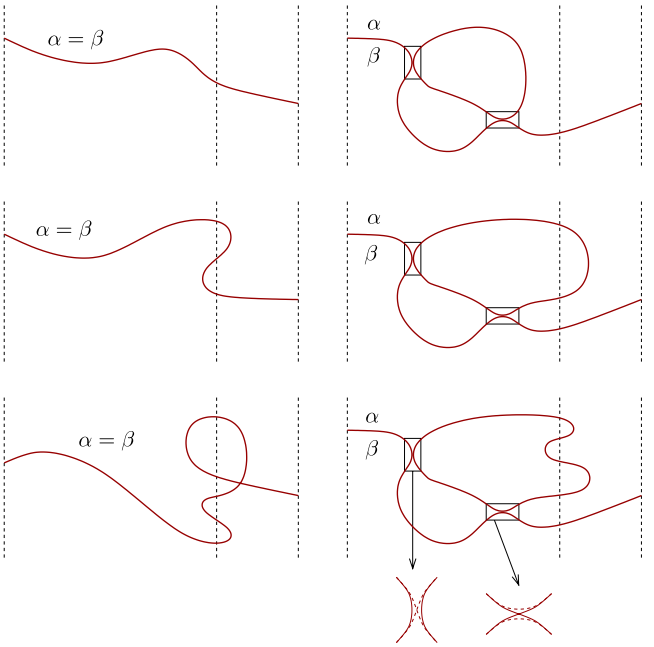

FIG. 8. (Color online) Examples of trajectory pairs contributing to the full average $\langle T(n)\rangle$ in the absence of time-reversal symmetry. The trajectory pairs have $m=1$ (top), $m=2$ (center), and $m=3$ (bottom). The left panel shows trajectory pairs without small-angle self intersections. The right panel shows trajectory pairs with two small-angle self intersections in the first $n-1$ cavities.

$$\langle \mathrm{tr}\, T(n)\rangle = \sum_{m=1}^{\infty} \frac{\langle \mathrm{tr}\, T(n-1)[\mathrm{tr}\, R(n-1)]^{m-1}\rangle}{2^m g_c^{m-1}} = \left\langle \frac{g_c\, \mathrm{tr}\, T(n-1)}{2g_c - \mathrm{tr}\, R(n-1)} \right\rangle. \tag{37}$$

A schematic representation of trajectory pairs contributing to Eq. (37) with up to two self-encounters in the first $n-1$ cavities are shown in Fig. 8. Using unitarity to express R in terms of T and subtracting $\langle \mathrm{tr}\, T(n-1)\rangle$, one then finds

$$\delta\langle \mathrm{tr}\, T(n)\rangle = \langle \mathrm{tr}\, T(n)\rangle - \langle \mathrm{tr}\, T(n-1)\rangle = \frac{1}{g_c}\langle [\mathrm{tr}\, T(n-1)]^2\rangle. \tag{38}$$

This is the same equation as one obtains from taking the average of the increment $\mathrm{tr}\, \delta T$ in the stochastic approach.

V. FIELD THEORY FORMULATION

In this section, we will approach the localization phenomenon from a different perspective. We will use that the quantum dot array depicted in Fig. 1 supports hierarchies of different types of field fluctuations in a field-theoretic description. These fluctuations reflect the fate of density distributions in classical phase space under the dynamical evolution of the system. Each of these fluctuations, thus, comes with a characteristic "relaxation time," i.e., a time scale on which the fluctuation decays. (For example, fluctuations inhomogeneous in the sector of phase space describing an in-

dividual quantum dot will decay on a time scale comparable to the time of flight through the dot, etc.) In the description of low energy phenomena such as the zero-frequency (dc) conductance, modes operating at short-time scales can be treated perturbatively. Their feedback into the sector of long-time scales then stabilizes a "low energy theory." In the following, we will derive a theory that is minimal in that it contains information equivalent to that stored in the Fokker-Planck equation of localization. The strategy pursued here parallels one applied previously[39] to the problem of dynamical localization in the quantum kicked rotor (also known as the "standard map"). One difference is that the spectrum of different modes encountered in the present problem happens to be more complex. Our logics also resemble that of Ref. 59, where it had been shown that the relevant low energy theory of an *ergodic* quantum system contains the information otherwise stored in random matrix theory.

Technically, our discussion will be based on a formulation of the array in terms of the ballistic nonlinear σ model.[60,61] A quadratic approximation in energetically high lying modes generates an effective low energy theory wherein each quantum dot is treated as a structureless ("ergodic") entity. This theory will be equivalent to the celebrated nonlinear σ model of disordered quantum wires,[62] a model that predicts Anderson localization on large length scales. We will see that the parameters stabilizing the hierarchical mode integration are the same as those utilized in previous sections of this paper.

Conceptually, the hierarchical scheme is an alternative to an indiscriminate perturbative integration over all modes in one go. That latter scheme would be essentially equivalent (see Ref. 59 for a discussion in the context of spectral statistics) to a semiclassical expansion in terms of paired trajectories. In this sense, the hierarchical mode integration processes the information stored in the statistics of trajectories by different means.

A. Field theory of the quantum dot array

Our starting point will be the description of the quantum dot array in terms of the supersymmetric ballistic nonlinear σ model. This theory is obtained by averaging exact functional representations of Green's functions over an energy interval of width ΔE centered around the uniform Fermi energy E_F of the array. A subsequent saddle-point approximation (stabilized in the parameter $E_F/\Delta E \gg 1$) then obtains a field theory in classical phase defined by

$$Z \equiv \int DT \exp(-S[T]), \tag{39}$$

with

$$S[T] = \frac{\beta\pi\hbar\nu}{2}\int_\Gamma (d\mathbf{x})\mathrm{tr}(T * \Lambda\{H, T^{-1}\}) + S_{\mathrm{reg}}[T]. \tag{40}$$

The integration variables in Eq. (39), $T(\mathbf{x})=\{T^{\alpha\alpha'}(\mathbf{x})\}$ are (super) matrix valued fields defined on shells $\Gamma=\{\mathbf{x}|H(\mathbf{x})=E_0\}$ of constant energy in classical phase space. Further, $\mathbf{x}\equiv(\mathbf{q},\mathbf{p})$ where $\mathbf{q}$ and $\mathbf{p}$ are coordinates and momenta, respectively, $H(\mathbf{x})$ is the Hamiltonian function of the system, the integral over the energy shell is normalized to the (spatial) volume of the system, $\int_\Gamma (d\mathbf{x}) = \mathrm{Vol}$, and ν is the single-particle density of states per volume, $\nu = 1/(\Delta \mathrm{Vol})$. For time-reversal and spin rotation invariant systems (orthogonal symmetry class, $\beta=1$), the "internal" structure of the matrices $T^{\alpha\alpha'}$ is described by a composite index $\alpha=(a,r,t)$, where $a=+/-$ discriminates between the advanced and retarded sector of the theory, $r=b,f$ discriminates between commuting and anticommuting sectors, and $t=1,2$ accounts for the operation of time reversal. Time reversal symmetry reflects in the relation $(\tau T^T \tau^{-1})(\mathbf{q},-\mathbf{p}) = T^{-1}(\mathbf{q},\mathbf{p})$, where τ is a fixed matrix whose detailed structure will not be of concern throughout. For time-reversal noninvariant systems (unitary symmetry, $\beta=2$), no time-reversal structure exists and $\alpha=(a,r)$. In either case, the matrices T carry a coset space structure in the sense that configurations T and TK are to be identified if $[K,\Lambda]=0$, where $\Lambda=\sigma_3^{\mathrm{ar}}$ and "ar" stands for action in advanced/retarded space. Finally, the regulatory action

$$S_{\mathrm{reg}}[T] \equiv \delta\int_\Gamma (d\mathbf{x})\mathrm{str}(\Lambda T^{-1} * \Lambda T), \quad \delta\downarrow 0$$

determines the "causality" of field fluctuations, but will otherwise not be of much relevance throughout.

The fluctuation behavior of the fields T in Eq. (39) is governed by the classical Liouville operator $\{H, \}$ (where $\{,\}$ is the Poisson bracket). Quantum mechanics enters the problem through the presence of Moyal products "$*$" in Eq. (39). In essence, this product operation[63] limits the maximum resolution of the theory in-phase space to scales of the order of a Planck cell. In Secs. V B and V C, we reduce the above "bare" theory to an effective low energy theory describing localization phenomena.

B. Hierarchical mode integration

Before turning to the technicalities of the mode integration, let us describe the relevant hierarchies in qualitative terms: fluctuations inhomogeneous in the phase-space sector representing individual dots are expected to relax on short-time scales comparable to the time of flight across the dot, t_f.[64] On the other hand, relative fluctuations in the configuration of different dots can survive up to time scales of the order of the dwell time $\tau_D \gg t_f$. To describe this hierarchical decay profile within our field theory framework, we focus on a section of the array containing two neighboring quantum dots (cf. Fig. 9). The fields $T(\mathbf{x})$ representing phase-space fluctuations in this subsystem may be decomposed as $T=T_sT_f$, where $T_{s,f}$ are "slow" and "fast" fluctuations, respectively. The slow fluctuations are (i) homogeneous within each dot separately. In particular, (ii) they do not vary in any spatial cross section transverse to the array, and (iii) do not depend on momentum. However, (iv) the weakness of the interdot coupling ($\tau_D \gg t_f$) leaves room for gradual fluctuations of the slow modes as we pass from one dot into the other. This suggests a parametrization $T_s(\mathbf{x})=T_s(q)$, where q is the component of $\mathbf{q}$ parallel to the longitudinal direction of the two-dot system. Point (i) above means that $T_s(q \ll 0)$

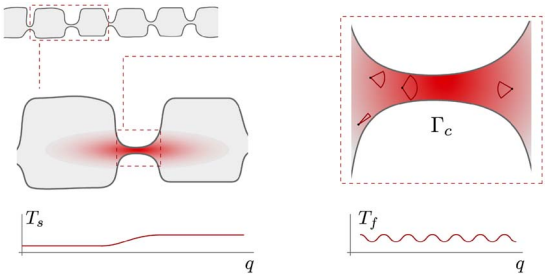

FIG. 9. (Color online) Top left: cartoon of an array of weakly coupled quantum dots. Center left: cut region containing two dots. The shaded region indicates the real-space support of the coupling phase space Γ_c. Bottom left: plot indicating the profile of weakly fluctuating field configurations: constancy throughout each dot, gradual variation in the coupling region. Center right: zoom into the coupling region. The phase-space region Γ_c contains points $\mathbf{x}=(\mathbf{q},\mathbf{n})$ that will migrate between the two dots in short time, i.e., without undergoing back scattering. (The opening angles represent those directions $\mathbf{n}$ that meet this criterion.) Bottom right: schematic plot of real-space profile of phase-space fluctuations generating the interdot coupling.

$=T_L$ and $T_s(q\gg 0)=T_R$, where $T_{L,R}$ are the constant slow mode configurations of the left and the right dot, respectively. As we are going to check in a self-consistent manner, (v) relative fluctuations between left and right dot are suppressed (in a parameter of the order of the number of transverse quantum channels supported by the connector region) so that a leading-order expansion in relative fluctuations $T_L T_R^{-1}$ is sufficient. (Conceptually, this expansion is equivalent to the Kramers-Moyal expansion employed in the derivation of the Fokker-Planck equation above.)

The field T_f encapsulates all other fluctuations, i.e., fluctuations that do not meet the criteria (i–v). Generic fluctuations of this type—think of fast fluctuations deep inside the phase space of one of the dots—are strongly gapped and do not couple to the slow fluctuations. (Formally, this decoupling manifests itself in an effective "orthogonality" between the modes representing these fluctuations.) However, there is one sector of phase space, Γ_c, in which fast and slow fluctuations talk to each other. The domain Γ_c includes all points in-phase space which pass from one dot to the other in a time of order $t_f \ll \tau_D$, much smaller than the typical dwell time (cf. the shaded area in Fig. 9). This region is special that it overlaps with the domain of gradual variation of the slow fields [cf. point (iv) above]. As we will see, a perturbative integration over fast fields in Γ_c effectively determines the slow field coupling between the two dots.

To prepare the integration over the fast fields in Γ_c, we need to bring the notation to a more explicit level: assuming that the bulk dynamics is ballistic, $\{H,\ \}=v_F\mathbf{n}\cdot\nabla$ where $\mathbf{n}$ is the unit vector in momentum space, and v_F the Fermi velocity. Current conservation in the specular reflection at the system boundaries translates to the effective boundary condition $f(\mathbf{x},\mathbf{n})=f(\mathbf{x},\bar{\mathbf{n}})$, where f is a phase function subject to the action of $\{H,\ \}$, $\mathbf{x}$ is a boundary point and $\bar{\mathbf{n}}$ is the direction vector with flipped normal component.

We next parametrize fluctuations as $T_{s,f}=\exp(W_{s,f})$, where the field generators carry a block structure (in advanced/retarded space),

$$W_{s,f}=\begin{pmatrix} & B_{s,f} \\ \bar{B}_{s,f} & \end{pmatrix}.$$

(For further technical details on this representation, we refer to Ref. 62.) We now substitute these generators into the action, expand to leading order in W_f, and integrate. This leads to the effective action

$$S_{\text{eff}}[T_s]=\frac{1}{2}\langle (S^{(1)}[T_s,W_f])^2\rangle + S_{\text{reg}}[T_s], \tag{41}$$

where $\langle\ldots\rangle\equiv\int DW_f \exp(-S^{(2)}[\mathbb{1},W_f])(\ldots)$, and $S^{(n)}[T_s,W_f]$ is of nth order in W_f. Due to the isotropy of T_s in momentum space and the linearity of the Poisson bracket in $\mathbf{n}$, the action does not contain a contribution of zeroth order in the fast fields. The dominant contribution to the coupling between fast and slow fluctuations is given by the linear term,

$$S^{(1)}[T_s,W_f]=\beta\pi\hbar\nu v_F\int_{\Gamma_c} d\mathbf{q}d\mathbf{n}n_{\parallel}\text{str}[W_s(\mathbf{q},\mathbf{n})\Phi(q)], \tag{42}$$

where we have introduced the abbreviation $\Phi\equiv(\partial_q T_s)*\Lambda T_s^{-1}$, the integration over the direction of momentum is normalized as $\int d\mathbf{n}=1$, $n_{\parallel}$ is the component of $\mathbf{n}$ parallel to the longitudinal direction and the Moyal product has been omitted [which is permissible due to the general relation $\int(d\mathbf{x})(f*g)(\mathbf{x})=\int(d\mathbf{x})(fg)(\mathbf{x})$ for the integrated product of *two* functions—presently, matrix elements of Φ and W—in phase space].

Neglecting contributions of $\mathcal{O}(\Phi W_f^2)$ [as compared to the $\mathcal{O}(\Phi W_f)$-terms above] the quadratic W_s-action is given by

$$S^{(2)}[T_s,W_f]\simeq S^{(2)}[\mathbb{1},W_f]=\beta\pi\hbar\nu\int_{\Gamma_c} d\mathbf{q}d\mathbf{n}\ \text{str}[\bar{B}_f(\mathbf{q},\mathbf{n})$$
$$\times(v_F\mathbf{n}\cdot\nabla+\delta)B_f(\mathbf{q},\mathbf{n})].$$

Fast field fluctuations can now be integrated out according to the prescription $\langle\text{str}[A(\mathbf{q},\mathbf{n})B_f(\mathbf{q},\mathbf{n})]\times\text{str}[\bar{A}(\mathbf{q}',\mathbf{n}')\bar{B}_f(\mathbf{q}',\mathbf{n}')]\rangle=\delta(\mathbf{n}-\mathbf{n}')\Pi(\mathbf{q},\mathbf{q}';\mathbf{n})$, where

$$\Pi(\mathbf{q},\mathbf{q}';\mathbf{n})\equiv\frac{1}{\beta\pi\hbar\nu}(v_F\mathbf{n}\cdot\nabla+\delta)^{-1}(\mathbf{q},\mathbf{q}').$$

Specifically, the effective action is given by

$$S_{\text{eff}}[T_s]=(\beta\pi\hbar\nu v_F)^2\int_{\Gamma_c} d\mathbf{q}d\mathbf{q}'d\mathbf{n}$$
$$\times n_{\parallel}^2\text{str}(\Phi_{21}(q)\Phi_{12}(q))\Pi(\mathbf{q},\mathbf{q}';\mathbf{n}).$$

So far, we have not made reference to the specific properties of the phase-space region Γ_c. We now assume that the corridor connecting the dots has waveguide properties, in that it (a) does not contain significant backscattering, and (b) the restriction of the Liouville operator to Γ_c has plane-wave-like eigenfunctions characterized by a conserved longitudinal/transverse momentum $\mathbf{k}_{\perp}/k$. We also assume that (c), the slow fields, smoothly interpolate between T_L and T_R in a region centered around the longitudinal coordinate $q=0$. The presumed proximity $T_L\simeq T_R$ implies that $\Phi(q)$

$\simeq \partial_q W(q)\Lambda$ can be linearized, where we suppressed the slow field index "s" for notational transparency. Under these circumstances, and noting that the integration over $\mathbf{q}_\perp$ implies a projection onto the zero-momentum sector $\mathbf{k}_\perp = 0$, we obtain

$$\begin{aligned} S_{\rm eff}[T_s] &= -\beta\pi\hbar\nu S_c v_F^2 \int_{-c}^{c} dq dq'\ \mathrm{str}[\Phi_{21}(q)\Phi_{12}(q')] \\ &\times \int d\mathbf{n} n_\parallel^2 \int \frac{dk}{2\pi} \frac{e^{ik(q-q')}}{i v_F n_\parallel k + \delta} \\ &= -\beta\pi\hbar\nu S_c v_F \int_{-c}^{c} dq dq'\ \mathrm{str}[\Phi_{21}(q)\Phi_{12}(q')] \\ &\times \int d\mathbf{n} |n_\parallel| \underbrace{\Theta\left(\frac{q-q'}{n_\parallel}\right)}_{=\text{const.}} \\ &= \text{const.} \times \hbar\nu S_c v_F\ \mathrm{str}[(\bar{B}_R - \bar{B}_L)(B_R - B_L)], \end{aligned}$$

where the indices refer to "ar"-space, const.$=\mathcal{O}(1)$ is a constant, S_c the transverse cross section of the contact, and $B_{R,L}$ are the generators of the slow fields in the left and the right dot, respectively. Noting that the density of states per volume, $\nu \sim m k_F^{d-2}$ (where $k_F = v_F m$ is the Fermi momentum) and $S_c k_f^{d-1} \sim N$ is proportional to the number of transverse channels, N, supported by the connector region, the prefactor can be written as const. $\times N \gg 1$, a number which we assume large lest a semiclassical description of the contact becomes meaningless. We also note that the quadratic form may be replaced by its unique rotationally invariant generalization to the full field manifold, $\mathrm{str}[(\bar{B}_R - \bar{B}_L)(B_R - B_L)] \to \frac{1}{4}\mathrm{str}(Q_L Q_R)$, where $Q = T\Lambda T^{-1}$. While a quadratic expansion of the latter expression reproduces the bilinear term, the largeness of N implies that typical values contributing to the B integration, $B \sim N^{-1/2} \ll 1$, which means that nonlinear contributions become inessential in the limit of large channel numbers. We thus conclude that the coupling term can be rewritten as

$$S_{\rm eff}[Q] = \text{const.} \times N\ \mathrm{str}(Q_L Q_R).$$

Finally, the obvious generalization of the above two-dot construction to an entire quantum dot array reads as

$$S_{\rm eff}[Q] = \text{const.} \times \frac{1}{\tau_D \Delta} \sum_m \mathrm{str}(Q_m Q_{m+1}), \tag{43}$$

where Q_m is the Q matrix representing the mth dot and we used that the channel number $N \sim (\tau_D \Delta)^{-1}$. Before turning to the discussion of localization properties, a few remarks on the construction above are in order.

Conceptually, the above reduction programs involves three steps: (1) identification of "low energy modes," i.e., modes that decay on the largest time scales of the problem, (2) identification of "high energy," or quickly decaying modes, and (3) perturbative integration over those fast modes that will conceivably couple to the slow modes. In principle, that integration can be explicated for any fluctuation in the problem. In practice, however, only few modes will effectively couple to the slow degrees of freedom, and these relevant fluctuations are best identified by semiclassical considerations:

(i) Semiclassically speaking, a "mode" represents the coherent propagation of a retarded and an advanced Feynman amplitude along classical trajectories in-phase space. Locally, the semiclassical dynamics of such composites is described by the Liouville operator, as is manifest in the action [Eq. (39)]. This trajectory interpretation helps in identifying the relevant fast modes. E.g., in the system depicted in Fig. 9, the coupling between the ergodic slow modes of each dot, Q_m, is dominated by trajectories swiftly propagating from one dot to the other, i.e., modes emanating at phase-space points $\mathbf{x} \in \Gamma_c$.

(ii) Although this identification of fast modes rests on specific model assumptions (no backscattering in the contact region, etc.), the result [Eq. (43)] is reasonably universal. For example, a somewhat more elaborate construction will show that the same action describes connector regions containing chaotic scattering and momentum relaxation by themselves. (The latter complication would manifest itself in an altered value of τ_D, though.) Generally speaking, the low energy physics of the system will reduce to $S_{\rm eff}$, as long as the dots are isolated from each other in the sense $t_f \ll \tau_D$.

C. Localization from the effective action (43)

The effective action (43) is equivalent to a "lattice version" of the diffusive nonlinear σ model of quasi-one-dimensional disordered wires. Indeed, we may pass to a continuum limit

$$\frac{1}{\tau_D \Delta} \sum_m \mathrm{str}(Q_m Q_{m+1}) \to \frac{a}{\tau_D \Delta} \int_0^L dx\ \mathrm{str}(\partial Q\, \partial Q),$$

where $Q_m \to Q(x)$ is replaced by a smooth field, $x = ma$, and a the spacing between the dots. Comparing to the standard form of the diffusive model,[62] where the action is $\sim \xi \int dx\ \mathrm{str}(\partial Q\, \partial Q)$ with ξ the localization length, we are led to the identification $\frac{a}{\tau_D \Delta} \sim \xi$.

VI. CONCLUSION

In the preceding sections, we showed how a theory of Anderson localization can be constructed for a sample in which the microscopic electron dynamics is ballistic, rather than disordered-diffractive. Our theory of ballistic Anderson localization paraphrases the scaling approach to localization in disordered quantum wires of Dorokhov[32] and Mello, *et al.*,[33] using the language of the trajectory-based semiclassical formalism. As noted in Sec. I, the interest of constructing such a semiclassical theory is not the structure of the theory itself or the phenomena it explains. Like most semiclassical theories of quantum corrections in the perturbative regime, the structure of the theory closely resembles the structure of its fully quantum-mechanical counterpart for disordered metals, whereas the observed phenomena are the same in the ballistic and disordered cases. Instead, the interest of the semiclassical theory is that it shows how quantum effects

that were known from disordered metals arise if the electron dynamics is ballistic.

On hindsight, it should not come as a surprise that a theory of ballistic Anderson localization can be constructed by adapting the derivation of the Dorokhov-Mello-Pereyra-Kumar equation for a disordered quantum wire. This point is best made by reconsidering Dorokhov's original derivation.[32] In this derivation, impurity scattering is treated in the Born approximation. All quantum-mechanical amplitudes are squared into quantum probabilities. Hence, it is sufficient if one can replace the quantum-mechanical probabilities by classical ones. Such a replacement is a standard procedure when connecting quantum-mechanical and semiclassical theories. Its implementation for the array of chaotic cavities is what is done here.

It is interesting to observe that, while small-angle encounters form a crucial link in our understanding of quantum interference corrections in ballistic conductors, their role is very limited in our description of localization in quasi-one-dimension: They serve to cancel spurious contributions from trajectories that enter the last cavity of the array more than twice. (In Dorokhov's original approach, such processes are excluded automatically because of the condition that the length of the wire is increased by an amount δL much smaller than the mean-free path l.[32,33]) Implicitly, small-angle encounters do play a much more important role in our theory, however, because they help to preserve unitarity in the semiclassical theory. Unitarity is a key ingredient of both the quantum-mechanical derivation of the DMPK equation and the present semiclassical derivation. We note that unitarity has played an important role in other extensions of the semiclassical framework beyond its previously assumed domain of validity: it is used to relate weak localization and enhanced backscattering, thus enabling a semiclassical description of weak localization without reference to small-angle encounters,[43,44,65] and it is used to obtain an alternative expression for the spectral form factor, allowing its calculation in the nonperturbative regime by considering periodic orbits of duration below the Heisenberg time only.[66]

We have also shown that the dynamical information entering the semiclassical approach can be processed by different means to derive an effective low energy field theory of the system. This latter approach is based on the concept of modes, fluctuations in-phase space decaying on parametrically different time scales. A successive integration over short-lived modes stabilizes an effective action of the most persistent modes in the fluctuation spectrum. In the present context, that low energy limit turned out to be equivalent to the diffusive nonlinear σ model of disordered wires. While the field theory approach is arguably less explicit than the direct classification of trajectories, it enjoys the advantage of high computational efficiency, a paradigm previously exemplified on the problem of universal spectral correlations.[59] For example, the above mentioned condition of unitarity, as well as the symmetries relating trajectories to their time reversed are built into the field theory approach from the outset; there is no need for explicit bookkeeping in terms of encounter processes. The price to be paid for this compactness in the description is a higher level of abstraction, though.

ACKNOWLEDGMENTS

We thank Fritz Haake for bringing this problem to our attention. This work was supported by the Packard Foundation, the Humboldt Foundation, the NSF under Grant No. DMR 0705476, and by the Sonderforschungsbereich SFB/TR 12 of the Deutsche Forschungsgemeinschaft.

[1] *Mesoscopic Quantum Physics*, edited by E. Akkermans, G. Montambaux, J.-L. Pichard, and J. Zinn-Justin (North-Holland, Amsterdam, 1995).

[2] Y. Imry, *Introduction to Mesoscopic Physics* (Oxford University, New York, 2002).

[3] P. W. Anderson, Phys. Rev. **109**, 1492 (1958).

[4] E. Abrahams, P. W. Anderson, D. C. Licciardello, and T. V. Ramakrishnan, Phys. Rev. Lett. **42**, 673 (1979).

[5] Exceptions to this rule include various one- and two-dimensional electron systems of non-Wigner-Dyson symmetry [see A. Altland and M. R. Zirnbauer, Phys. Rev. B **55**, 1142 (1997)], and two-dimensional systems with spin-orbit scattering. For a discussion of the localization properties of these systems we refer to F. Evers and A. D. Mirlin, arXiv:0707.4378 (unpublished). However, the quasi-one-dimensional systems studied in this work categorically show localization.

[6] A. D. Stone, in *Mesoscopic Quantum Physics*, edited by E. Akkermans, G. Montambaux, J.-L. Pichard, and J. Zinn-Justin (North-Holland, Amsterdam, 1995).

[7] K. Nakamura and T. Harayama, *Quantum Chaos and Quantum Dots* (Oxford University, New York, 2004).

[8] This expectation holds only if the relevant electronic time scales exceed the "Ehrenfest time," the minimum time after which quantum effects appear in ballistic conductors; see Ref. 42.

[9] F. Haake, *Quantum Signatures of Chaos* (Springer, New York, 1991).

[10] L. P. Kouwenhoven, C. M. Marcus, P. L. McEuen, S. Tarucha, R. M. Westervelt, and N. S. Wingreen, in *Mesoscopic Electron Transport*, NATO Advanced Studies Institute Series E: Applied Science Vol. 345, edited by L. L. Sohn, L. P. Kouwenhoven, and G. Schön (Kluwer, Dordrecht, 1997).

[11] M. L. Roukes and A. Scherer, Bull. Am. Phys. Soc. **34**, 633 (1989).

[12] K. Ensslin and P. M. Petroff, Phys. Rev. B **41**, 12307 (1990).

[13] M. Gutzwiller, *Chaos in Classical and Quantum Mechanics* (Springer, New York, 1990).

[14] W. H. Miller, Adv. Chem. Phys. **25**, 69 (1974).

[15] R. Blümel and U. Smilansky, Phys. Rev. Lett. **60**, 477 (1988).

[16] R. A. Jalabert, H. U. Baranger, and A. D. Stone, Phys. Rev. Lett. **65**, 2442 (1990).

[17] M. Sieber and K. Richter, Phys. Scr. **T90**, 128 (2001).

[18] M. Sieber, J. Phys. A **35**, L613 (2002).

[19] K. Richter and M. Sieber, Phys. Rev. Lett. **89**, 206801 (2002).

[20] S. Müller, S. Heusler, P. Braun, and F. Haake, New J. Phys. **9**, 12 (2007).
[21] The relation between quantum corrections and small-angle encounters of classical trajectories was first discovered by Aleiner and Larkin in a formalism which allowed the classical dynamics to be modified by quantum effects, instead of expressing quantum phenomena in terms of classical trajectories only; see Refs. 28 and 42.
[22] S. Müller, S. Heusler, P. Braun, F. Haake, and A. Altland, Phys. Rev. Lett. **93**, 014103 (2004).
[23] S. Müller, S. Heusler, P. Braun, F. Haake, and A. Altland, Phys. Rev. E **72**, 046207 (2005).
[24] S. Heusler, S. Müller, P. Braun, and F. Haake, Phys. Rev. Lett. **96**, 066804 (2006).
[25] R. S. Whitney and P. Jacquod, Phys. Rev. Lett. **96**, 206804 (2006).
[26] P. W. Brouwer and S. Rahav, Phys. Rev. B **74**, 075322 (2006).
[27] D. Cohen, J. Phys. A **31**, 277 (1998).
[28] I. L. Aleiner and A. I. Larkin, Phys. Rev. E **55**, R1243 (1997).
[29] M. V. Berry, Proc. R. Soc. London, Ser. A **400**, 229 (1985).
[30] S. Heusler, S. Müller, A. Altland, P. Braun, and F. Haake, Phys. Rev. Lett. **98**, 044103 (2007).
[31] This expectation has been verified using numerical simulations in the context of "Dynamic localization" (Ref. 36), Anderson localization in momentum space rather than in real space, which is relevant for certain dynamic systems with a periodic time-dependent Hamiltonian; see Refs. 37 and 38.
[32] O. N. Dorokhov, Pis'ma Zh. Eksp. Teor. Fiz. **36**, 259 (1982) [JETP Lett. **36**, 318 (1982)].
[33] P. A. Mello, P. Pereyra, and N. Kumar, Ann. Phys. (N.Y.) **181**, 290 (1988).
[34] K. B. Efetov and A. I. Larkin, Zh. Eksp. Teor. Fiz. **85**, 764 (1983) [Sov. Phys. JETP **58**, 444 (1983)].
[35] K. B. Efetov, Adv. Phys. **32**, 53 (1983).
[36] S. Fishman, D. R. Grempel, and R. E. Prange, Phys. Rev. Lett. **49**, 509 (1982).
[37] G. Casati, B. V. Chirikov, J. Ford, and F. M. Izrailev, Lect. Notes Phys. **93**, 334 (1979).
[38] D. L. Shepelyansky, Phys. Rev. Lett. **56**, 677 (1986).
[39] A. Altland and M. R. Zirnbauer, Phys. Rev. Lett. **77**, 4536 (1996).
[40] V. L. Berezinskii, Zh. Eksp. Teor. Fiz. **65**, 1251 (1973) [Sov. Phys. JETP **38**, 620 (1974)].
[41] H. Schanz and U. Smilansky, Phys. Rev. Lett. **84**, 1427 (2000).
[42] I. L. Aleiner and A. I. Larkin, Phys. Rev. B **54**, 14423 (1996).
[43] H. U. Baranger, R. A. Jalabert, and A. D. Stone, Phys. Rev. Lett. **70**, 3876 (1993).
[44] H. U. Baranger, R. A. Jalabert, and A. D. Stone, Chaos **3**, 665 (1993).
[45] A. D. Mirlin, A. Müller-Groeling, and M. R. Zirnbauer, Ann. Phys. (N.Y.) **236**, 325 (1994).
[46] P. W. Brouwer and K. Frahm, Phys. Rev. B **53**, 1490 (1996).
[47] C. W. J. Beenakker, Rev. Mod. Phys. **69**, 731 (1997).
[48] M. R. Zirnbauer, Phys. Rev. Lett. **69**, 1584 (1992).
[49] This need not be immediately obvious if time-reversal symmetry is present ($\beta=1$), since Eq. (5) contains the matrix G^q, which cannot be expressed in terms of T^q. Still, the stochastic process defined by Eqs. (4) fully describes the evolution of the eigenvalues of $\mathcal{T}^q$, which can be verified by considering the mean change of $\mathrm{tr}(T^q)^m$ or of a product of such traces, which contains G^q in the combination $G^q(T^*)^n G^{q\dagger} = (T^q)^{n+2} - (T^q)^{n+3}$ only, $n = 0, 1, 2, \ldots$.
[50] A. V. Tartakovski, Phys. Rev. B **52**, 2704 (1995).
[51] P. W. Brouwer, Phys. Rev. B **57**, 10526 (1998).
[52] B. Rejaei, Phys. Rev. B **53**, R13235 (1996).
[53] We prefer to use a formulation with continuous momenta p and p' instead of one with discrete momenta, as used in most of the semiclassical literature. For each set trajectory that contributes to the conductance, there exists a large number ($\sim g_c$) of sets of deformed trajectories that have different momenta upon entrance and exit. The difference between a momentum sum and a momentum integral disappears if $g_c \gg 1$.
[54] D. Spehner, J. Phys. A **36**, 7269 (2003).
[55] M. Turek and K. Richter, J. Phys. A **36**, L455 (2003).
[56] S. Rahav and P. W. Brouwer, Phys. Rev. B **73**, 035324 (2006).
[57] P. W. Brouwer, Phys. Rev. B **76**, 165313 (2007).
[58] P. W. Brouwer and S. Rahav, Phys. Rev. B **74**, 085313 (2006).
[59] J. Müller, T. Micklitz, and A. Altland, Phys. Rev. E **76**, 056204 (2007).
[60] B. A. Muzykantskiĭ and D. E. Khmelnitskiĭ, Pis'ma Zh. Eksp. Teor. Fiz. **62**, 68 (1995) [JETP Lett. **62**, 76 (1995)].
[61] A. V. Andreev, B. D. Simons, O. Agam, and B. L. Altshuler, Nucl. Phys. B **482**, 536 (1996).
[62] K. B. Efetov, *Supersymmetry in Disorder and Chaos* (Cambridge University, Cambridge, 1997).
[63] The Moyal product between two phase space functions A and B is defined as $(A*B)(\mathbf{x}) = \exp(\frac{1}{2} i\hbar \partial_{\mathbf{x}'}^T I \partial_{\mathbf{x}}^{\boldsymbol{\delta}}) A(\mathbf{x}')B(\mathbf{x})|_{x=x'}$, where I is the symplectic unit matrix.
[64] In fact, the phase space of individual dots supports a small set of fluctuations that decay on time scales longer than the generic t_f: the probability $\Pi(\mathbf{x}, \bar{\mathbf{x}}', t)$ to propagate from a phase space point $\mathbf{x}$ to the time reversed of a closeby point $\mathbf{x}'$ relaxes on scales $\sim \lambda^{-1} \ln(E_F t_f / us)$, where λ is the dominant Lyapunov exponent of the system and s and u are the locally most stable and unstable coordinate of the point $\mathbf{x}'$ in a coordinate system that has $\mathbf{x}$ as its center. Since the phase space resolution of the quantum theory is limited by $us \sim \hbar$, these long-time memory effects decay on time scales of the order of the Ehrenfest time $\tau_E \sim \lambda^{-1} \ln(S/us)$. Thus, the decoupled dots have relaxed into a fully ergodic configuration on time scales $\tau_E < \tau_D$.
[65] N. Argaman, Phys. Rev. Lett. **75**, 2750 (1995).
[66] J. P. Keating and S. Müller, Proc. R. Soc. London, Ser. A **463**, 3241 (2007).